Cosmogenic nuclides in Almahata Sitta ureilites: Cosmic-ray exposure age, preatmospheric mass, and bulk density of asteroid 2008 TC3

K. C. Welten* M. M. M. Meier† M. W. Caffee‡
K. Nishiizumi** R. Wieler††
P. Jenniskens‡‡ M. H. Shaddad§

*
†
‡
**
††
‡‡
§

The Meteoritical Society

Meteoritics & Planetary Science 45, Nr 10–11, 1728–1742 (2010)
doi: 10.1111/j.1945-5100.2010.01106.x

Cosmogenic nuclides in Almahata Sitta ureilites: Cosmic-ray exposure age, preatmospheric mass, and bulk density of asteroid 2008 TC_3

Kees C. WELTEN[1*], Matthias M. M. MEIER[2], Marc W. CAFFEE[3], Kuni NISHIIZUMI[1], Rainer WIELER[2], Peter JENNISKENS[4], and Muawia H. SHADDAD[5]

[1]Space Sciences Laboratory, University of California, Berkeley, California 94720–7450, USA
[2]Department of Earth Sciences, ETH Zürich, CH-8092 Zürich, Switzerland
[3]PRIME Laboratory, Purdue University, West Lafayette, Indiana 47907, USA
[4]Carl Sagan Center, SETI Institute, 515 North Whisman Road, Mountain View, California 94043, USA
[5]Department of Physics and Astronomy, University of Khartoum, P.O. Box 321, Khartoum 11115, Sudan
[*]Corresponding author. E-mail: kcwelten@berkeley.edu

(Received 24 December 2009; revision accepted 04 August 2010)

Abstract–On October 7, 2008, a small F-class asteroid, 2008 TC_3, exploded in Earth's atmosphere, and produced a strewn field of meteorites in the Nubian Desert of Sudan. Subsequent searches yielded several hundred meteorite fragments, known as Almahata Sitta. This fall was classified as a polymict ureilite. We measured cosmogenic radionuclides in six fragments and noble gases in four fragments of the Almahata Sitta ureilite. The concentrations of ^{10}Be, ^{26}Al, and ^{36}Cl in the meteorite fragments of asteroid 2008 TC_3 indicate a preatmospheric radius of 300 ± 30 g cm^{-2}. Combined with an absolute radius of 1.8 ± 0.2 m, which was derived from its brightness in space, the cosmogenic radionuclides constrain the bulk density of asteroid 2008 TC_3 to 1.66 ± 0.25 g cm^{-3} and the bulk porosity to 50 ± 7%. The bulk density of asteroid TC_3 is on the low end of the range of 1.6–3.3 g cm^{-3} determined for 40 of the recovered ureilite fragments. Since the denser materials have a higher chance of surviving atmospheric fragmentation, the low-density ureilites are probably more representative of the bulk asteroid. We thus conclude that the high porosity of asteroid 2008 TC_3 is mainly due to microporosity, which implies that not all low-density asteroids are necessarily rubble pile structures. Finally, from the cosmogenic ^{21}Ne concentrations, we determined a cosmic-ray exposure (CRE) age of 19.5 ± 2.5 Myr. This age represents the time since asteroid 2008 TC_3 was ejected from a large F-class parent body in the asteroid belt, until its collision with Earth.

INTRODUCTION

On October 6, 2008, a small asteroid, 2008 TC_3, was discovered to be on a collision course with Earth (Kowalski et al. 2008). Less than 20 h later, the roughly 4 m large asteroid exploded in the atmosphere at an altitude of 37 km above the Nubian Desert of northern Sudan. In December 2008, a search party led by two of us (PJ and MS) recovered 47 fragments of this meteorite. Several consecutive expeditions increased the total to more than 600 fragments with a total mass of approximately 10.5 kg (Shaddad et al. 2010). The meteorite, known as Almahata Sitta, was classified as an anomalous polymict ureilite (Jenniskens et al. 2009) and is described in more detail in several other papers in this issue. Since its classification as a polymict ureilite, several chondritic fragments have also been identified in the strewn field, which are believed to be part of the same object and further emphasize that Almahata Sitta is a unique polymict breccia (Bischoff et al. 2010; Shaddad et al. 2010). Since the reflectance spectrum of 2008 TC_3 is consistent with F-class asteroids, the discovery of the surviving meteorite fragments of Almahata Sitta firmly links ureilites to F-class objects in the asteroid belt. The most likely origin of these F-class asteroids is either the Polana family, which is located near the 3:1 resonance (Cellino et al. 2001; Jenniskens et al. 2010), or the Hoffmeister

family, which is located near the 5:2 resonance (Migliorini et al. 1996).

The preatmospheric size and shape of Almahata Sitta was determined from direct observations of asteroid 2008 TC_3 in the last few hours before impact (Scheirich et al. 2010). The shape of the asteroid is oblong, with axes of approximately 2.4, 3.6, and 6.6 m, corresponding to a volume of 25 ± 10 m^3 and an effective radius of approximately 1.8 m (Scheirich et al. 2010). The volume of 25 m^3 is based on an average albedo of 0.049 ± 0.010 for F-class asteroids (Warner et al. 2009), which is consistent with the measured albedo of 0.046 ± 0.005 for one of the recovered meteorites (Jenniskens et al. 2009). Subsequent albedo measurements on 10 Almahata Sitta ureilite fragments yield a mean albedo of 0.088 ± 0.015 (Hiroi et al. 2010). An albedo of approximately 0.09 lowers the effective radius of the asteroid to 1.3–1.4 m, which corresponds to a volume of approximately 10 m^3 and a mass of < 30,000 kg. This low estimate of the preatmospheric mass does, however, seem inconsistent with the amount of energy released during the atmospheric fragmentation of asteroid 2008 TC_3 (Borovička and Charvat 2009). While the distinction between meteoroids and asteroids as a function has ranged from 1 to 10 m, the recent discovery of asteroid 2008 TC_3 by telescopes led Rubin and Grossman (2010) to define asteroids as objects with a minimum size of approximately 1 m.

Additional constraints on the size of asteroid 2008 TC_3 came from the measured kinetic energy in light output and infrasound (Jenniskens et al. 2009), all pointing to an effective radius of approximately 2 m and a mass of approximately 80,000 kg, the latter with an uncertainty of approximately 50%. The acoustic signals from the fireball detected at the Kenyan infrasonic array corresponded to an energy of $(6.7 \pm 2.1) \times 10^{12}$ J. Analysis of the bolide light curve shows a total radiated energy of about 4×10^{11} J, which translates to a preatmospheric kinetic energy of about 4×10^{12} J (Borovička and Charvat 2009). With an entry speed of 12.4 km s^{-1} (at 100 km), these values translate to a pre-entry mass between 35,000 and 65,000 kg. Based on the high altitude at which asteroid 2008 TC_3 broke up in the atmosphere, Borovička and Charvat (2009) estimate a bulk porosity of approximately 50%.

While asteroid 2008 TC_3 was in space as a meter-sized object, it was exposed to cosmic rays, resulting in the production of stable and radioactive cosmogenic nuclides. The production rates of these cosmogenic nuclides in the Almahata Sitta meteorites are functions of the preatmospheric size and mass of the meteoroid, the irradiation depth of samples within the meteoroid, and the chemical composition of the samples. The concentrations of stable cosmogenic nuclides in Almahata Sitta are a measure of its cosmic-ray exposure (CRE) age, i.e., the time between ejection from a shielded position on its much larger (km-sized) parent body and impact on Earth. The concentrations of cosmogenic radionuclides provide information on the shielding conditions of the samples during irradiation. Although the preatmospheric size of the Almahata meteorites is relatively well constrained from the astronomical observations, the preatmospheric mass has a larger uncertainty since the bulk density of the object is unknown. The measured densities of the recovered ureilite fragments show large variations, ranging from 1.6 to 3.3 g cm^{-3} (Shaddad et al. 2010), suggesting that the small asteroid was quite heterogeneous. The average density of 40 surviving meteorite fragments is approximately 2.8 g cm^{-3}, but it is not clear whether this value is representative of the bulk density of asteroid 2008 TC_3. In this work, we report the concentrations of cosmogenic radionuclides and noble gases in six Almahata Sitta ureilite fragments, to determine the preatmospheric mass of asteroid 2008 TC_3, thus constraining its bulk density and porosity, and to determine its CRE age.

SAMPLE SELECTION AND EXPERIMENTAL METHODS

Sample Selection

We received small chips of six ureilitic Almahata Sitta fragments (#1, #4, #15, #36, #44, and #47), of which four (#4, #36, #44, and #47) were also large enough for noble gas analysis. These samples come from different positions in the Almahata Sitta strewn field, representing almost the full range of the 29 km long area surveyed so far. Sample #1 (4.4 g) represents the low-mass (<10 g) end of the field, while samples #15 (75 g) and #36 (58 g) traveled up to 22 km further East, representing the high-mass end of the strewn field. The selected ureilite samples show densities ranging from 1.77 to 3.11 g cm^{-3} (Shaddad et al. 2010). Aliquots of our chips of meteorite fragments #4 and #47 were also analyzed for oxygen isotopes (Rumble et al. 2010), mineralogy/petrography (Zolensky et al. 2010), and chemical composition by inductively coupled plasma–mass spectrometry (ICP-MS) (Friedrich et al. 2010). For sample #4, the carbon content was determined by A. Steele (personal communication). Short-lived radionuclides were measured in the main mass of sample #15 (Taricco et al. 2010). Cosmogenic and trapped noble gases were measured in aliquots of samples #1 and #47 (Ott et al. 2010).

Table 1. Concentrations of major elements (in wt%) in Almahata Sitta ureilite samples. Concentrations of Mg, Al, Ca, Mn, Fe, and Ni were measured by atomic absorption spectrometry, while O, Si, and the partitioning of Fe between FeNi and FeO were estimated (values in italics, see text). Measured bulk densities of meteorite fragments are from Shaddad et al. (2010).

Sample	ρ (g cm^{-3})	Mass (mg)	O	Mg	Al	Si	Ca	Mn	Fe	Ni	FeNi	FeO
#1	1.77 ± 0.17	69.9	*37*	19.6	0.16	*19*	0.92	0.28	20.8	0.37	*13.5*	*9.0*
#4	2.55 ± 0.08	117.6	*42*	20.9	0.29	*22*	1.72	0.38	9.7	0.05	*1.3*	*10.8*
#15	3.11 ± 0.02	39.8	*39*	17.0	0.43	*20*	5.75	0.32	15.2	0.14	*6.0*	*11.6*
#36	2.67 ± 0.02	123.5	*43*	23.7	0.17	*21*	1.12	0.31	7.6	0.03	*0.0*	*9.7*
#44	–	99.1	*40*	19.5	0.28	*21*	1.73	0.30	14.6	0.16	*6.2*	*10.7*
#47	2.96 ± 0.05	122.6	*40*	20.1	0.14	*21*	1.05	0.28	15.1	0.17	*6.6*	*10.7*

Estimated values of bulk O, Si, FeNi-metal, and FeO are in italics.

Cosmogenic Radionuclides

We crushed aliquots of 40–125 mg to < 0.5 mm. For the analysis of long-lived cosmogenic radionuclides ^{10}Be (half-life = 1.36×10^6 yr), ^{26}Al (7.05×10^5 yr), and ^{36}Cl (3.01×10^5 yr), we dissolved samples in a mixture of concentrated HF/HNO_3 along with a carrier solution containing 3–5 mg of Be and Cl. After dissolution, Cl was isolated as AgCl, and the remaining solution was evaporated to dryness using $HClO_4$. The residue was dissolved in 0.5N HCl and a small aliquot was taken for chemical analysis by atomic absorption spectroscopy (AAS) before adding 2.8–5.5 mg of Al carrier to the remaining solution. The Al content of the meteorite samples (0.14–0.43 wt%) contributes 2–5% of the total Al used for radionuclide analysis. Results of the chemical analysis are shown in Table 1. We separated Be and Al and measured the concentrations of ^{10}Be, ^{26}Al, and ^{36}Cl by accelerator mass spectrometry (AMS) at Purdue University (Sharma et al. 2000). After subtracting blank levels, we normalized the measured isotopic ratios to ^{10}Be, ^{26}Al, and ^{36}Cl AMS standards (Sharma et al. 1990; Nishiizumi 2004; Nishiizumi et al. 2007). The quoted errors in Table 2 represent 1σ uncertainties in the AMS measurements of the samples, blanks and standards, but not the uncertainty in the absolute value of the standards (which is the same for all samples).

Noble Gases

The concentrations and isotopic compositions of light noble gases were measured in chips (#4, #36, #44, and #47) of 30–150 mg in a single extraction step at 1800 °C, following procedures described previously (Wieler et al. 1989). Results are shown in Table 3. Uncertainties in the measured concentrations are on the order of 4–6%, while uncertainties in the isotopic ratios are approximately 1%. Helium and argon are a mixture of cosmogenic, trapped and radiogenic components, while neon only consists of cosmogenic and trapped components.

Helium

Measured ^{4}He/^{3}He ratios range from 6.5 to 11.6, somewhat higher than the average cosmogenic ^{4}He/^{3}He ratio of approximately 6 (Alexeev 1998; Welten et al. 2003). Although the cosmogenic ^{4}He/^{3}He ratio varies somewhat as a function of shielding (Reedy 1981), the elevated ^{4}He/^{3}He ratios in Almahata Sitta indicate the presence of small contributions of trapped and/or radiogenic ^{4}He, ranging from 20 to 150×10^{-8} cm^3 STP g^{-1}. Even if all noncosmogenic ^{4}He were trapped, with $(^3\text{He}/^4\text{He})_{tr} = 1.4 \times 10^{-4}$ (Rai et al. 2003), the corrections for trapped ^{3}He are still negligible (< 0.1%) in all samples. Accordingly, all ^{3}He is taken to be cosmogenic. No reliable concentrations of radiogenic ^{4}He concentrations can be reported for any of our samples, because of uncertain corrections for trapped He. However, if we assume a cosmogenic ^{4}He/^{3}He ratio of 6 and a trapped ^{4}He/^{20}Ne ratio of approximately 20, then we can constrain radiogenic ^{4}He to $< 50 \times 10^{-8}$ cm^3 STP g^{-1} in all samples. These low radiogenic ^{4}He concentrations are consistent with the low U and Th concentrations reported by Friedrich et al. (2010) in two of our samples (#4 and #47).

Neon

The measured ^{20}Ne/^{22}Ne ratios in Almahata Sitta fragments #4 and #36 are approximately 0.87, only slightly above the cosmogenic ratio of approximately 0.83, indicating a small contribution of trapped Ne. The ^{20}Ne/^{22}Ne ratios of 0.96–1.75 in the other two fragments indicate slightly larger trapped Ne contributions, with $^{20}Ne_{tr}$ in the range of $(1.1–7.1) \times 10^{-8}$ cm^3 STP g^{-1}. Corrections for trapped Ne were made assuming Ne is a mixture of cosmogenic Ne with ^{20}Ne/^{22}Ne = 0.83 (Eberhardt et al. 1965) and ureilite-Ne with ^{20}Ne/^{22}Ne = 10.4 (Ott 2002).

Argon

Measured ^{36}Ar/^{38}Ar ratios for all Almahata samples are close to the value of approximately 5.3 for trapped Ar in ureilites (Göbel et al. 1978). Because of

Table 2. Concentrations of cosmogenic ^{10}Be, ^{26}Al, and ^{36}Cl (in dpm kg^{-1}) in Almahata Sitta ureilites. The last column shows normalized ^{36}Cl concentrations (in dpm kg^{-1} [Fe*]), in which Fe* = Fe + 12Ca.

Sample	^{10}Be	^{26}Al	^{36}Cl	Fe*	^{36}Cl*
#1	19.0 ± 0.4	43.8 ± 0.9	5.9 ± 0.2	31.8	18.6 ± 0.6
#4	22.5 ± 0.9	56.6 ± 1.9	5.4 ± 0.1	30.3	17.8 ± 0.4
#15	19.6 ± 0.4	60.0 ± 2.0	15.3 ± 0.5	84.2	18.2 ± 0.6
#36	21.9 ± 0.4	55.1 ± 2.3	3.6 ± 0.1	21.0	17.3 ± 0.5
#44	21.4 ± 0.4	49.0 ± 1.9	6.1 ± 0.1	35.4	17.2 ± 0.4
#47	24.1 ± 0.9	55.8 ± 1.6	5.6 ± 0.1	27.7	20.1 ± 0.5

Table 3. Measured concentrations (in 10^{-8} cm^3 STP g^{-1}) and isotopic ratios of light noble gases in Almahata Sitta ureilites. The measured ^{36}Ar/^{38}Ar ratios are too close to the value of trapped Ar of approximately 5.35 to allow an accurate calculation of cosmogenic ^{38}Ar, which are thus not shown. Measured ^{36}Ar is essentially identical to the concentration of trapped ^{36}Ar and measured ^{40}Ar is a mixture of radiogenic and atmospheric Ar. The last two columns show the trapped ^{4}He and ^{20}Ne concentrations based on cosmogenic ratios of ^{4}He/^{3}He = 6 and ^{20}Ne/^{22}Ne = 0.83.

Sample	Mass (mg)	^{3}He	^{4}He	^{21}Ne	^{22}Ne	^{20}Ne/^{22}Ne	^{36}Ar	^{40}Ar	^{4}He	^{20}Ne$_{tr}$
#4a	29.0	22.0	144	6.93	7.37	0.870	32.4	139.0	12	0.3
#4b	52.2	22.0	144	7.09	7.53	0.872	29.0	84.0	11	0.3
#36	47.0	24.2	171	7.25	7.73	0.870	13.1	97.7	25	0.3
#44	71.4	27.0	315	5.80	7.08	1.752	1390	84.1	152	7.1
#47a	32.0	27.6	251	7.66	8.26	1.041	108	154.0	85	1.9
#47b	147.7	28.1	222	8.01	8.42	0.964	84.0	126.0	53	1.1

Uncertainties in measured concentrations are on the order of 4–6%.

the large trapped argon component, no attempt was made to calculate the cosmogenic ^{38}Ar concentrations. All six Almahata Sitta samples contain very low ^{40}Ar concentrations (84–154 × 10^{-8} cm^3 STP g^{-1}), which show no correlation with trapped ^{36}Ar. Although most of the trapped Ar in Almahata Sitta has a ureilitic composition with an average trapped ^{40}Ar/^{36}Ar ratio of 0.002 (Rai et al. 2003), we cannot exclude that the samples, which were in the Nubian desert for several months before being discovered, contain small contributions of trapped atmospheric Ar with a ^{40}Ar/^{36}Ar ratio of 296. We thus conclude that the measured ^{40}Ar concentrations are upper limits for the radiogenic ^{40}Ar component, which cannot be determined reliably. The low radiogenic ^{40}Ar concentrations are consistent with the low K concentrations (<5 ppm) in Almahata Sitta.

RESULTS AND DISCUSSION

Chemical Composition

The six fragments of Almahata Sitta show large variations in bulk composition (Table 1), most notably in Al (0.14–0.43 wt%), Ca (0.9–5.8 wt%), Fe (7.6–20.8 wt%), and Ni (0.03–0.37%), while Mg, Si, and Mn are relatively constant, and K is below our detection limit (approximately 5 ppm). The variations in Al, Ca, Fe, and Ni are similar to those reported in four fragments analyzed by ICP-MS (Friedrich et al. 2010). They are also comparable to variations in chemical composition between individual fragments of another polymict ureilite shower, Frontier Mountain 90036 (Welten et al. 2006). In addition, comparison of the chemical composition of fragments #4, #15, and #47 analyzed by Friedrich et al. (2010) with our data shows that the major element concentrations in Almahata Sitta show considerable scatter for different aliquots of the same fragments, implying that the Almahata Sitta polymict ureilite is quite heterogeneous even on a mm to cm scale.

The concentrations of Ni show a positive correlation with those of Fe, yielding a slope of approximately 0.025 (Fig. 1). This correlation is most likely due to the presence of variable amounts of metal with an average Ni content of 2.5 wt%. This low Ni content is consistent with kamacite compositions of other ureilites, which have an average kamacite-Ni content of approximately 2 wt% (Berkley et al. 1980) and with kamacite-Ni contents of 1.3–4.5 wt% measured in Almahata Sitta (Hoffmann et al. 2010). From the measured Fe and Ni concentrations in the Almahata Sitta samples, we estimate bulk metal contents of 0–13 wt% (Table 1). These large variations in metal content are consistent with the wide range of magnetic susceptibilities found in ureilite falls and finds

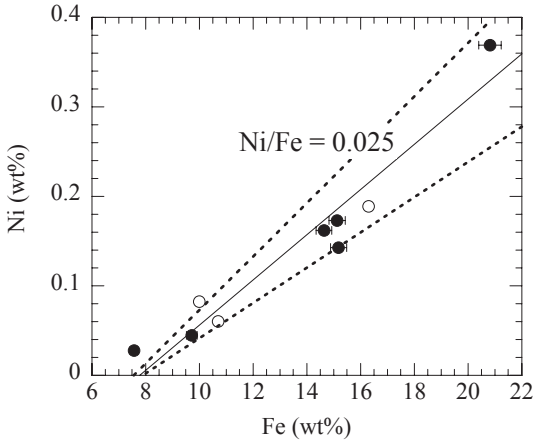

Fig. 1. Relationship of Ni and Fe in Almahata ureilites, with closed symbols representing AAS data from this work, open symbols ICP-MS data from Friedrich et al. (2010). The solid line represents a linear fit through the data, yielding a slope of 0.025 ± 0.005, indicating that most of the data are consistent with a mixture of silicates (containing approximately 8 wt% Fe and < 0.01 wt% Ni) plus 0–13 wt% metal (kamacite) with Ni contents of 2–3 wt%.

(Rochette et al. 2009). The metal in Almahata Sitta is mainly present as micron-sized particles (Hoffmann et al. 2010). Fragment #1 has the highest metal content combined with the lowest bulk density. This observation is consistent with the hypothesis of Herrin et al. (2009) that the reduction of Fe, Mg-silicates by C produced metallic Fe, SiO_2, and CO, in which the production of CO gas presumably led to the high porosity and thus the low density of fragment #1.

In general, bulk SiO_2 contents of achondrites can be derived from the elemental analysis of Mg, Al, Ca, Cr, Mn, Fe, and Ni, by assuming that these elements are present as oxides, using SiO_2 = 100% – [sum of all oxides]. This method yields SiO_2 contents of 36 wt% (sample #1) to 46 wt% (sample #4) for the Almahata Sitta samples. However, if we take into account that part of the Fe (and all of the Ni) is present as kamacite, the method yields SiO_2 contents of 40–47 wt%. We used the latter method to estimate bulk Si and O contents for Almahata Sitta samples (Table 1). The large variations in chemical composition have significant effects on the cosmogenic nuclide production rates.

Cosmogenic Radionuclide Concentrations

The measured concentrations of ^{10}Be, ^{26}Al, and ^{36}Cl in the six Alamahata Sitta samples are functions of the chemical composition and the shielding condition of each sample. Since all Almahata Sitta samples came from the same object, the shielding condition simply refers to the irradiation depth of the samples within asteroid 2008 TC_3. We will first discuss the observed variations in cosmogenic ^{10}Be, ^{26}Al, and ^{36}Cl as a function of chemical composition and shielding effects and then use the entire data set to derive the preatmospheric size of the Almahata Sitta meteorite.

The ^{10}Be concentrations of 19.0–24.1 dpm kg^{-1} in Almahata Sitta are typical of average-sized ureilites with radii of 100–300 g cm^{-2} (Aylmer et al. 1990), indicating that ^{10}Be is at or near saturation, which requires a minimum CRE age of approximately 5 Myr. Figure 2a shows that the observed variations in ^{10}Be are mainly due to variations in shielding, as shown by the relationship between ^{10}Be and the shielding dependent ^{22}Ne/^{21}Ne ratio, which generally decreases with increasing shielding. The lowest ^{10}Be concentration (19 dpm kg^{-1}) is found in sample #1, which experienced low shielding, as indicated by its ^{22}Ne/^{21}Ne ratio of approximately 1.12 (Ott et al. 2010), while ^{10}Be concentrations of 22–24 dpm kg^{-1} are found in samples #4, #36, and #47, which show ^{22}Ne/^{21}Ne ratios of approximately 1.05, indicative of high shielding depths. The low ^{10}Be concentration of 19.5 dpm kg^{-1} in sample #15 does not seem to be due to low shielding, because the high ^{26}Al concentration in sample #15 (Fig. 2b) suggests high shielding. While cosmogenic ^{10}Be in most stone meteorites is mainly produced from O, Mg, and Si, with small contributions from Fe, ^{10}Be in ureilites is also produced from carbon, which varies from 0–5 wt% in ureilites. With typical ^{10}Be production rates of 100–150 atoms min^{-1} kg^{-1} for C and 20–25 atoms min^{-1} kg^{-1} for silicates (Nagai et al. 1993; Leya and Masarik 2009), the ^{10}Be concentration in ureilites can vary by 20–30% due to variations in carbon. To date, the bulk C content of only one Almahata Sitta sample (#4) has been measured, yielding a value of 2.2 ± 0.3 wt% C (A. Steele, unpublished). Based on the dark color of most Almahata ureilite fragments (including sample #4), we assume that most samples contain approximately 2 wt% carbon, while sample #15 is much lighter in color and probably contains <1 wt% carbon. We thus conclude that the low ^{10}Be concentration in fragment #15 is most likely due to its low bulk C content. Although variations in O (37–43 wt%), Mg (17–24 wt%), and Si (19–22 wt%) may have also contributed to the observed variations in ^{10}Be, these effects are small compared to those due to shielding and bulk carbon.

The ^{26}Al concentrations in the Almahata fragments range from approximately 44 dpm kg^{-1} in sample #1 to approximately 60 dpm kg^{-1} in sample #15. Since the main target elements for ^{26}Al production (Si and Al) are relatively constant in the Almahata Sitta ureilites, variations in chemical composition only have a small effect (<10% variation) on the ^{26}Al production rate.

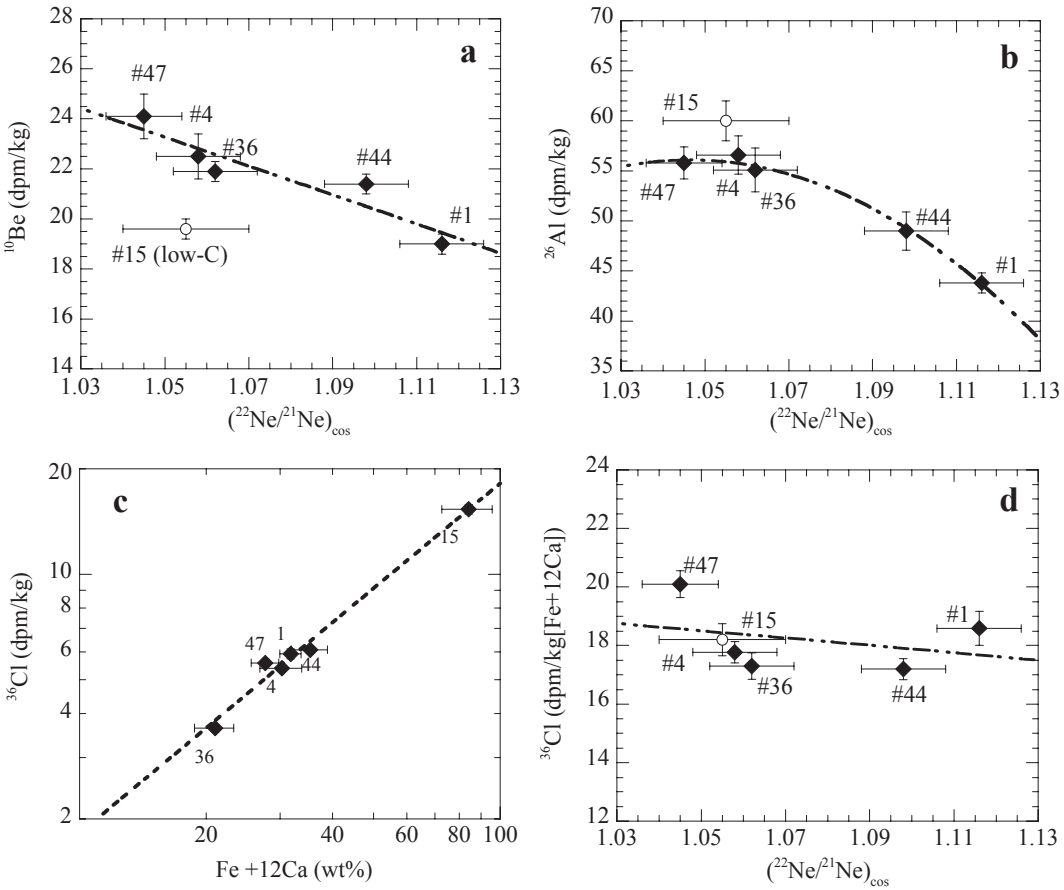

Fig. 2. Relationship between a) ^{10}Be, b) ^{26}Al, and c–d) ^{36}Cl in six Almahata Sitta fragments versus the cosmogenic ^{22}Ne/^{21}Ne ratio, which decreases with increasing shielding. Figure (c) shows a linear dependence of the measured ^{36}Cl concentrations on the major target elements, Fe and Ca, assuming $P(^{36}Cl)_{Ca}/P(^{36}Cl)_{Fe} = 12$. Normalized ^{36}Cl concentrations in (d) are based on the observed correlation in (c). Measured $(^{22}Ne/^{21}Ne)_{cos}$ ratios for #4, #36, #44, and #47 are from this work, while the value for #1 is from Ott et al. (2010). The $(^{22}Ne/^{21}Ne)_{cos}$ ratio for #15 is assumed to be 1.055 ± 0.015, the average value of the three most shielded samples. The scale of the *y*-axis of (a, b, d) is chosen so that all three plots show a factor of 2 variation in radionuclide concentration.

Figure 2b shows a negative correlation between ^{26}Al concentration and the shielding sensitive ^{22}Ne/^{21}Ne ratio, i.e., samples #1 and #44, which have ^{22}Ne/^{21}Ne ratios of 1.10–1.12, show low ^{26}Al concentrations, while the remaining samples, with ^{22}Ne/^{21}Ne ratios of 1.04–1.07, show relatively constant ^{26}Al concentrations of 57 ± 2 dpm kg^{-1}. This correlation implies that the observed variations in ^{26}Al are mainly due to shielding effects, with low ^{26}Al concentrations representing samples near the surface (<50 g cm^{-2} shielding) and high ^{26}Al concentrations representing samples near the center (>50 g cm^{-2} shielding) of asteroid 2008 TC$_3$.

The cosmogenic ^{36}Cl concentrations in Almahata Sitta range from 3.6 to 15.3 dpm kg^{-1}, mainly due to variations in Fe and Ca, the main target elements for ^{36}Cl production. Cosmogenic ^{36}Cl concentrations in the Almahata Sitta samples show a linear correlation with the effective Fe concentration, Fe* = Fe + 12Ca (Fig. 2c), assuming that the elemental production rate of ^{36}Cl from Ca is 12 times higher than that from Fe, i.e., $P(^{36}Cl)_{Ca}/P(^{36}Cl)_{Fe} = 12$. This assumption is consistent with calculated $P(^{36}Cl)_{Ca}/P(^{36}Cl)_{Fe}$ ratios of 10–15 for most depths in moderately large meteorites (Leya and Masarik 2009). Although small amounts of ^{36}Cl are produced from Ti, Cr, and Mn, the total contributions from these minor elements are small (1–3%) compared to those from Fe and Ca, and we therefore ignored them. After normalization to the major target elements, the bulk ^{36}Cl concentrations yield a relatively constant normalized ^{36}Cl concentration of 18.2 ± 1.1 dpm kg[Fe + 12Ca]$^{-1}$, which shows almost no dependence on shielding, as shown by the negligible slope of ^{36}Cl as a function of the cosmogenic ^{22}Ne/^{21}Ne ratio (Fig. 2d).

In summary, we conclude that the observed variations in ^{36}Cl are mainly due to variations in the

main target elements, Fe and Ca, while the variations in ^{10}Be and ^{26}Al are mainly due to shielding effects. The dependence of the measured radionuclide concentrations as a function of preatmospheric size are discussed below.

Preatmospheric Size

To match the measured radionuclide concentrations in the Almahata Sitta ureilites with calculated depth profiles, we used elemental production rates of ^{10}Be, ^{26}Al, and ^{36}Cl for carbonaceous chondrites (CC) with radii of 85–200 cm (Leya and Masarik 2009). Since the average density of asteroid 2008 TC_3 is unknown, we plot the production rates as a function of depth expressed in g cm^{-2}, a unit that is commonly used for cosmogenic nuclide depth profiles. Based on a density of 2.25 g cm^{-3} for CC, radii of 85–200 cm correspond to values of 190–450 g cm^{-2}. We used a bulk ureilite composition of 2 wt% C, 40.2 wt% O, 20.8 wt% Mg, 20.7 wt% Si, 1.3 wt% Ca, and 13.6 wt% Fe + Ni, the average composition of Almahata Sitta #1, #4, #36, #44, and #47. We assume that the elemental production rates are insensitive to differences in bulk composition between ureilites and chondrites. This seems a reasonable assumption given that the Fe content of the most Fe-rich Almahata Sitta ureilite (20.8 wt%) overlaps with that of CI and CM chondrites (18.5–21.0 wt%). We are aware that the model calculations of Leya and Masarik (2009) are in principle only valid for spherical objects, while observations of asteroid 2008 TC_3 indicate that this object was far from spherical (Scheirich et al. 2010). Preliminary model calculations on the effect of meteoroid shape indicates that production rates in nonspherical objects are somewhat lower than in spherical objects with the same volume (Masarik and Reedy 1994a; Kim et al. 2005), suggesting that we may overestimate production rates in asteroid 2008 TC_3 by approximately 10%, but this does not significantly affect our conclusions. Calculated depth profiles of ^{10}Be, ^{26}Al, and ^{36}Cl in ureilites with radii of 190–450 g cm^{-2} are shown in Fig. 3. For meteorites with CRE ages >10 Myr, the radionuclide concentrations are in saturation, which implies that the measured concentrations (in dpm kg^{-1}) are equal to the production rates (in atoms min^{-1} kg^{-1}).

Figure 3a shows that the measured ^{10}Be concentrations of 21–24 dpm kg^{-1} in #4, #36, #44, and #47 show best agreement with calculated ^{10}Be production rates in an object with a radius of approximately 270 g cm^{-2}. However, this conclusion is somewhat dependent on the assumed bulk carbon content of 2 wt%, which was measured in only one of the samples and may vary from 0 to 5 wt% in other Almahata samples. Lower bulk carbon contents result in lower ^{10}Be production rates and thus a smaller radius, while higher bulk carbon contents would lead to higher ^{10}Be production rates and thus a larger radius for asteroid 2008 TC_3. Therefore, the ^{10}Be data alone only constrain the radius of asteroid 2008 TC_3 to 225–340 g cm^{-2}.

The correlation between ^{26}Al and ^{22}Ne/^{21}Ne (Fig. 2b) shows that ^{26}Al in Almahata Sitta is more shielding dependent than ^{10}Be, with ^{26}Al concentrations of 44–49 dpm kg^{-1} near the surface and concentrations of 55–60 dpm kg^{-1} near the center of the preatmospheric object. Figure 3b shows that ^{26}Al concentrations in the near-surface samples provide little information on the preatmospheric size of Almahata Sitta, because they are consistent with production rates for near-surface locations in objects with radii of 190–450 g cm^{-2}. However, the relatively constant ^{26}Al concentrations of 55–60 dpm kg^{-1} in the four more shielded samples provide a better constraint for the preatmospheric radius. According to the model calculations, objects smaller than 270 g cm^{-2} in radius yield ^{26}Al production rates of 60–70 dpm kg^{-1} at depths >50 g cm^{-2}, while objects larger than 340 g cm^{-2} show ^{26}Al production rates of <55 dpm kg^{-1} at depths >50 g cm^{-2}. The measured ^{26}Al concentrations in the four most shielded Almahata Sitta ureilites thus constrain the preatmospheric radius to 270–340 g cm^{-2}, with a value of approximately 300 g cm^{-2} as the best fit.

Figure 3c shows a comparison of the measured ^{36}Cl concentrations in Almahata Sitta with calculated ^{36}Cl depth profiles using elemental production rates for CC from Leya and Masarik (2009). Both the measured ^{36}Cl concentrations and calculated ^{36}Cl production rates were normalized to the effective Fe concentration, Fe*, as described above. The measured ^{36}Cl concentrations in Almahata Sitta seem to constrain the radius of asteroid 2008 TC_3 to <270 g cm^{-2} (Fig. 3c). However, the ^{36}Cl depth profiles in Fig. 3c only include spallation reactions, and do not take contributions from capture of thermal neutrons on ^{35}Cl into account, which may be significant as thermal neutron fluxes reach a maximum in objects with a radius of approximately 300 g cm^{-2} (Spergel et al. 1986).

The neutron-capture rates of ^{36}Cl in large objects are strongly dependent on (1) depth in the meteoroid, (2) the macroscopic neutron capture cross section of the meteoroid, and (3) the native Cl concentration (Spergel et al. 1986). Although the Cl concentrations in Almahata Sitta are unknown, ureilites typically have Cl contents in the range of 0–15 ppm (Garrison et al. 2000). Based on an average macroscopic neutron cross section, $\sum_{eff} = 0.059 \pm 0.013$ for Almahata Sitta compositions, compared to $\sum_{eff} = 0.085$ for average L

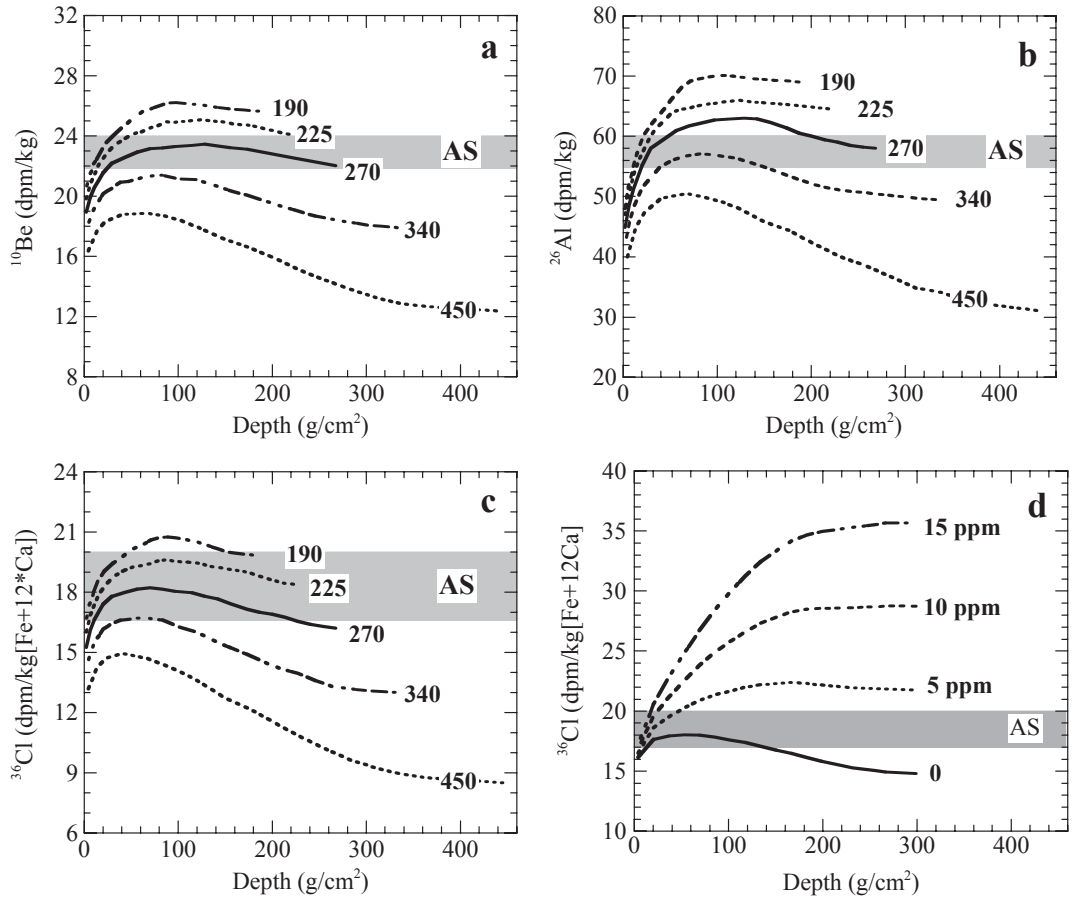

Fig. 3. Calculated depth profiles of a) ^{10}Be, b) ^{26}Al, c) spallogenic ^{36}Cl, and d) spallogenic + neutron-capture ^{36}Cl in asteroid 2008 TC_3, for radii of 190–450 g cm^{-2}. Calculations are based on the elemental production rates in carbonaceous chondrites from Leya and Masarik (2009), neutron-capture rates for R = 300 g cm^{-2} (Spergel et al. 1986), and the average chemical composition of Almahata Sitta ureilites assuming 2 wt% carbon (a) and 0–15 ppm Cl (d). The gray bars in each figure represent the range of measured concentrations in samples #4, #15, #36, and #47 (excluding sample #15 for ^{10}Be). The measured concentrations and calculated production rates of ^{36}Cl (c, d) were normalized to an effective Fe concentration, Fe* = Fe + 12Ca.

chondrite composition (Lingenfelter et al. 1972), we estimate that neutron-capture rates in Almahata Sitta are approximately 45% higher than in L chondrites of the same size (in g cm^{-2}). Expected neutron-capture rates for ^{36}Cl in the center of an ureilitic object with a radius of 300 g cm^{-2} are thus on the order of approximately 360 dpm g^{-1}Cl, i.e., intermediate between those for chondrites (approximately 250 dpm g^{-1}Cl) and those for aubrites (approximately 1000 dpm g^{-1}Cl). We used the depth profile of Spergel et al. (1986), normalized to ureilite compositions to calculate neutron capture ^{36}Cl production rates for Cl contents of 0–15 ppm and added the neutron-capture ^{36}Cl contributions to the calculated spallogenic ^{36}Cl depth profiles of Fig. 3c. Figure 3d shows that even Cl concentrations of a few ppm can result in significant contributions of neutron-capture ^{36}Cl in the center of an object with R = 300 g cm^{-2}. This implies that the measured ^{36}Cl concentrations in Almahata Sitta are consistent with a radius of approximately 300 g cm^{-2} if we assume Cl contents of 1–3 ppm. We can also turn this argument around, concluding that independent of the exact size of asteroid 2008 TC_3 (as long as it is in the range of 200–400 g cm^{-2}), the measured ^{36}Cl concentrations in the Almahata Sitta ureilites constrain their Cl content to <5 ppm.

In summary, based on the measured ^{10}Be, ^{26}Al, and ^{36}Cl concentrations in the Almahata Sitta ureilites, in comparison with calculated production rates of Leya and Masarik (2009), we conclude that asteroid 2008 TC_3 had a radius of 300 ± 30 g cm^{-2}.

Bulk Density and Porosity

From the absolute radius of asteroid 2008 TC_3 (R, in cm), as determined from the brightness in space and

Table 4. Preatmospheric size, mass, density and porosity of asteroid 2008 TC_3, based on a radius of 300 g cm^{-2} derived from cosmogenic radionuclides, and absolute radii of 128–202 cm, based on the absolute magnitude of 30.9, and an average albedo ranging from 0.04 to 0.10. The radius of 180 cm for $a = 0.05$ is based on a volume of 25 m^3 determined by Scheirich et al. (2010).

Albedo	Radius (cm)	Density (g cm^{-3})	Volume (m^3)	Mass (10^3 kg)	Porosity (vol%)
0.040	202	1.49	34.3	51.1	56
0.050	180	1.66	24.6	40.9	50
0.060	165	1.82	18.7	34.1	46
0.070	152	1.97	14.8	29.2	41
0.080	143	2.10	12.1	25.5	37
0.090	134	2.23	10.2	22.7	33
0.100	128	2.35	8.7	20.4	30

its albedo, and its radius (r, in g cm^{-2}), as determined from the cosmogenic radionuclides, we can determine the bulk density, using $\rho = r/R$. The absolute radius of asteroid 2008 TC_3 is somewhat dependent on the average albedo (a), with reported values of the Almahata Sitta ureilites ranging from $a = 0.046$ (Jenniskens et al. 2009) to a = approximately 0.09 (Hiroi et al. 2010), which are both within the range of typical albedos of 0.04–0.10 for F-class objects (Jenniskens et al. 2010). The corresponding radius of 2008 TC_3 ranges from 134 cm (for $a = 0.09$) to approximately 200 cm (for $a = 0.04$), based on an absolute volume of 25 m^3 for $a = 0.05$ (Scheirich et al. 2010). For the purpose of this study we assume an albedo of 0.05 ± 0.01, which corresponds to a radius of 180 ± 20 cm. Combining the absolute radius of 180 ± 20 cm with the radius of 300 ± 30 g cm^{-2} derived from cosmogenic radionuclides, yields a density of 1.66 ± 0.25 g cm^{-3} and a preatmospheric mass of (41 ± 8) × 10^3 kg (Table 4). The preatmospheric mass is below the range of (83 ± 25) × 10^3 kg determined initially (Jenniskens et al. 2009), but consistent with more recent estimates of (50 ± 15) × 10^3 kg (Borovička and Charvat 2009).

The density of approximately 1.7 g cm^{-3} for asteroid 2008 TC_3 is approximately 40% lower than the average density of approximately 2.8 g cm^{-3} determined for 40 Almahata ureilite fragments (Fig. 4a), representing approximately 2.6 kg of the recovered meteorite. However, it is within the observed range of 1.6–3.2 g cm^{-3} for these meteorites (Shaddad et al. 2010). Based on an average mineral grain density of approximately 3.35 g cm^{-3} for ureilites (Britt and Consolmagno 2003), the bulk density of 1.66 ± 0.25 g cm^{-3} of asteroid 2008 TC_3 indicates a porosity of

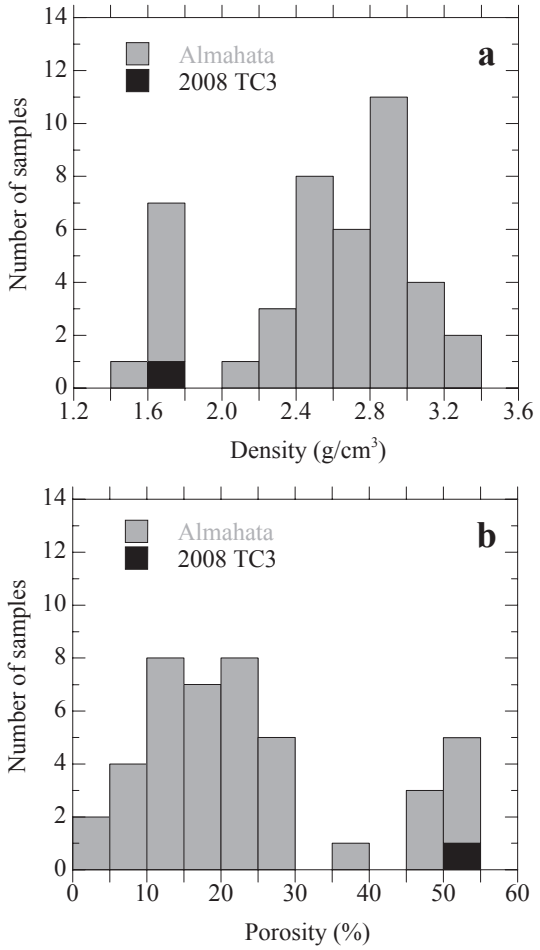

Fig. 4. a) Bulk density and b) and bulk porosity of asteroid 2008 TC_3 as determined from cosmogenic radionuclide concentrations in Almahata Sitta meteorites and the absolute radius of approximately 1.8 m (see text) in comparison with measured densities and inferred porosities of individual meteorite fragments from the Almahata Sitta ureilite strewn field. The histograms do not include the densities or porosities of nonureilitic Almahata Sitta meteorite fragments (Shaddad et al. 2010).

50 ± 7%. This porosity is higher than porosities of approximately 40% measured in some of the meteorite fragments (Zolensky et al. 2009), but is remarkably similar to (but more accurate than) the estimate of approximately 50% based on the altitude at which the object exploded in the atmosphere (Borovička and Charvat 2009). The higher average density of the recovered meteorites relative to the bulk meteoroid indicates that the denser materials have a higher probability of surviving atmospheric fragmentation.

If we would assume an albedo of approximately 0.09 (Hiroi et al. 2010) for asteroid 2008 TC_3, then we would obtain a bulk density of approximately 2.2 g cm^{-3}, a porosity of 33%, and a total mass of

Table 5. Cosmic-ray exposure ages (T3, T21) of Almahata Sitta ureilite based on concentrations (in 10^{-8} cm^3 STP g^{-1}) of cosmogenic ^{3}He and ^{21}Ne and production rates (P3 and P21, in 10^{-8} cm^3 STP g^{-1} Myr^{-1}) of ^{3}He and ^{21}Ne based on equations from Eugster (1988) and Aylmer et al. (1990). The columns labeled P3′ and P21′ show chemical correction factors based on the chemical composition of the Alamahata Sitta samples, compared to average L chondrite composition. The last column shows the ^{21}Ne-^{26}Al ages, assuming ^{21}Ne/^{26}Al production rate ratios (in units of [10^{-10} cm^3 STP g^{-1} Myr^{-1}]/[dpm kg^{-1}]) of 0.67 for samples #4, #36, and #47 and 0.64 for sample #44.

Sample	^{3}He$_c$	^{21}Ne$_c$	(^{3}He/^{21}Ne)$_c$	(^{22}Ne/^{21}Ne)$_c$	P3′	P21′	P3	P21	T3	T21	P (^{21}Ne)/P(^{26}Al)	T (^{21}Ne-^{26}Al)
#4a	22.0	6.93	3.17	1.059	1.05	1.30	1.71	0.500	12.9	13.9	0.67 ± 0.01	19.3 ± 1.9
#4b	22.0	7.09	3.11	1.056	1.05	1.30	1.71	0.506	12.9	14.0		
#36	24.2	7.25	3.34	1.062	1.06	1.44	1.72	0.544	14.1	13.3	0.67 ± 0.01	18.0 ± 1.8
#44	27.0	5.78	4.66	1.098	1.03	1.22	1.66	0.386	16.3	15.0	0.64 ± 0.02	19.6 ± 2.0
#47a	27.6	7.66	3.60	1.054	1.03	1.24	1.68	0.489	16.5	15.6	0.67 ± 0.01	21.1 ± 2.1
#47b	28.1	8.01	3.51	1.036	1.03	1.24	1.68	0.531	16.7	15.1		

23,000 kg (Table 4). Although the density of 2.2 g cm^{-3} is within the range of densities measured for the Almahata ureilites, the total mass seems inconsistent with the amount of energy released during atmospheric disruption (Borovička and Charvat 2009), so we prefer the lower albedo, which yields a lower density, a higher porosity, and a larger mass (Table 4). Note that—independent of the average albedo—the derived density of 1.7–2.2 g cm^{-2} overlaps within empirical uncertainties with the density of approximately 2 g cm^{-3} reported for one of the main F-class objects, asteroid 142 Polana (Jenniskens et al. 2010). This does not necessarily mean that 142 Polana is the parent body of asteroid 2008 TC$_3$, but that F-class objects like asteroid 142 Polana could be the parent body.

Noble Gases and CRE Age

The cosmogenic ^{3}He and ^{21}Ne concentrations and the cosmogenic ^{3}He/^{21}Ne and ^{22}Ne/^{21}Ne ratios are shown in Table 5. Concentrations (in units of 10^{-8} cm^3 STP g^{-1}) are relatively constant at 22–28 (^{3}He$_c$) and 5.8–8.0 (^{21}Ne$_c$), respectively. The mean values of the two splits of sample #47 obtained here are 10–12% higher than the respective values of a split of #47 analyzed by Ott et al. (2010), while the ^{3}He$_c$ and ^{21}Ne$_c$ concentrations in our sample #36 are 4% higher and 19% lower, respectively, than the corresponding values measured by Murty et al. (2010) in a different split of the same specimen. This is reasonable agreement in view of the rather small sample size and the chemical heterogeneity of the Almahata Sitta samples. Also the shielding-sensitive ratio, (^{22}Ne/^{21}Ne)$_{cos}$, is quite constant (around 1.05–1.06) in all samples except sample #44 (this work) and #1 (Ott et al. 2010). Both samples have a (^{22}Ne/^{21}Ne)$_{cos}$ ratio of approximately 1.10, indicating that they were closer to the preatmospheric surface than the others. The shielding-dependence of the (^{22}Ne/^{21}Ne)$_{cos}$ ratio in ureilites is less well constrained than that for chondrites, but for "average-sized" ureilites this ratio is about 2% lower at a given position than it would be at the same position in an L chondrite, due to approximately 20% higher Mg/(Mg + Al + Si) ratios in ureilites (Aylmer et al. 1990; Masarik and Reedy 1994b). In a Bern-type plot of ^{3}He/^{21}Ne versus ^{22}Ne/^{21}Ne, both normalized to L chondrite composition (Fig. 5), the Almahata samples plot close to the Bern-line, indicating no significant loss of ^{3}He. The chondrite-renormalized value of the (^{22}Ne/^{21}Ne)$_{cos}$ ratio for most of our samples is about 1.06–1.08, just at the lower end of the range for which it can reasonably be used for shielding correction (Leya et al. 2000). However, the (^{22}Ne/^{21}Ne)$_{cos}$ ratio in large objects is not always a reliable shielding parameter, as has been shown before (e.g., Welten et al. 2003). We therefore used two different methods to calculate the CRE age.

In the first method, production rates are calculated according to the formalism of Eugster (1988), describing the dependence of ^{3}He and ^{21}Ne production rates in chondrites as a function of (^{22}Ne/^{21}Ne)$_{cos}$, again after taking into account that the (^{22}Ne/^{21}Ne)$_{cos}$ ratios in ureilites are systematically approximately 2% lower than in L chondrites. We used chemical correction factors P3′ (for ^{3}He production) and P21′ (for ^{21}Ne production) for each individual sample, since the major element concentrations in the Almahata Sitta ureilite vary significantly from sample to sample (Table 1). Calculated ^{3}He and ^{21}Ne production rates for the given chemical compositions and (^{22}Ne/^{21}Ne)$_{cos}$ ratios are listed in Table 5. This method yields ^{3}He ages ranging from 12.9 to 16.7 Myr (average = 14.9 ± 1.8 Myr) and ^{21}Ne ages of 13.3–15.6 Myr (average = 14.5 ± 0.9 Myr) (Fig. 6).

In the second method we use elemental production rates from Leya and Masarik (2009) for chondritic

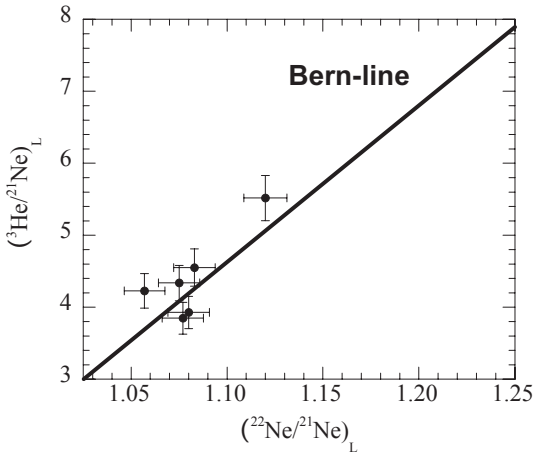

Fig. 5. The correlation of cosmogenic $^3He/^{21}Ne$ versus $^{22}Ne/^{21}Ne$ ratios for Almahata Sitta ureilites, after normalization to L chondrite composition. The solid line represents the correlation of $^3He/^{21}Ne$ versus $^{22}Ne/^{21}Ne$ for chondrites, known as the Bern-line (Eberhardt et al. 1966). The correlation is from Nishiizumi et al. (1980).

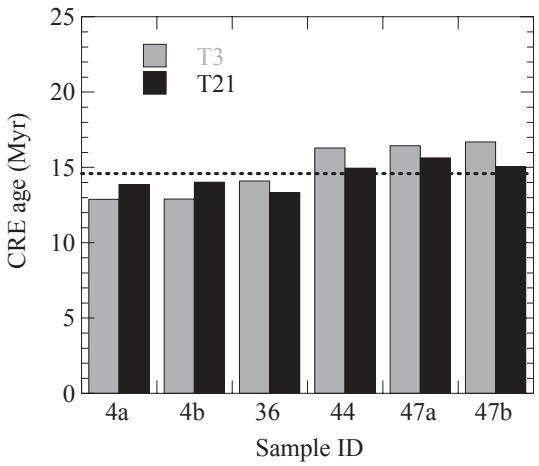

Fig. 6. Cosmic-ray exposure (CRE) ages of Almahata Sitta samples #4 (two aliquots), #36, #44, and #47 (two aliquots). CRE ages, T3 and T21, were calculated from the measured ^3He and ^{21}Ne concentrations and ^3He and ^{21}Ne production rates as a function of the cosmogenic $^{22}Ne/^{21}Ne$ ratio (Eugster 1988; Aylmer et al. 1990).

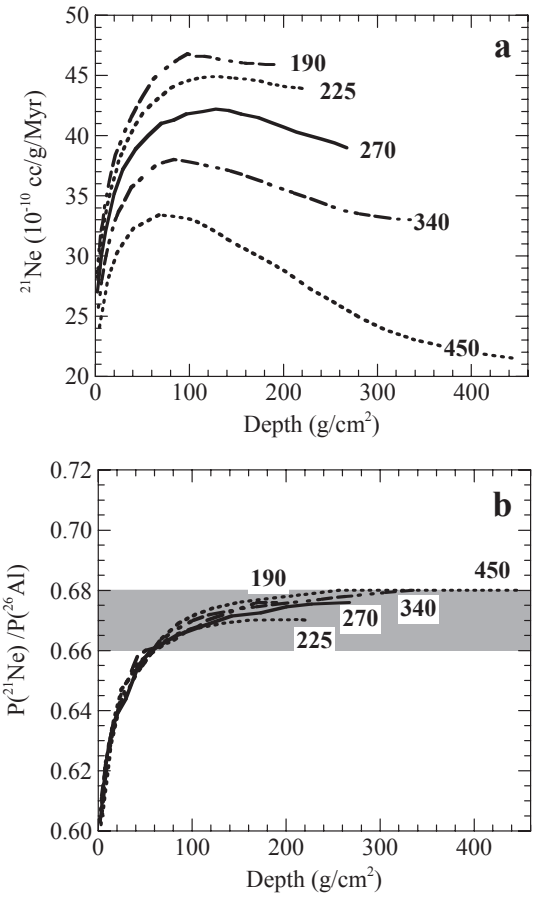

Fig. 7. Calculated depth profiles of a) the ^{21}Ne production rate (in units of 10^{-10} cm^3 STP g^{-1} Myr^{-1}) and b) the $^{21}Ne/^{26}Al$ production rate ratio (in units of [10^{-10} cm^3 STP g^{-1} Myr^{-1}]/[dpm kg^{-1}]) in ureilites with radii of 190–450 g cm^{-2} and the chemical composition of Almahata Sitta. The gray bar in (b) highlights the relatively constant $^{21}Ne/^{26}Al$ production rate ratio for depths >50 g cm^{-2} in objects with radii of 190–450 g cm^{-2}.

objects with radii of 190–450 g cm^{-2} to calculate the ^{21}Ne production rate (Fig. 7a) and the $^{21}Ne/^{26}Al$ production rate ratio (Fig. 7b). Previous studies and model calculations (e.g., Graf et al. 1990) have shown that in stone meteorites, the $^{21}Ne/^{26}Al$ ratio is relatively independent of shielding conditions and chemical composition. For example, the CRE age of 107 Myr for the large Norton County aubrite, based on the $^{21}Ne/^{26}Al$ method (Herzog and Anders 1971), is still valid today (Lorenzetti et al. 2003). Figure 7b shows that the calculated $^{21}Ne/^{26}Al$ production rate ratio increases from approximately 0.64 near the surface (approximately 20 g cm^{-2}) to 0.67 ± 0.01 for depths >50 g cm^{-2}. Using a $^{21}Ne/^{26}Al$ production rate ratio of 0.64 ± 0.02 for the near surface sample (#44) and a ratio of 0.67 for sample #4, #36, and #47, we calculate CRE ages of 18–21 Myr, with an average of 19.5 ± 1.5 Myr (Table 5). This age is significantly higher than the ^3He and ^{21}Ne ages of 13–17 Myr, confirming that simple shielding corrections based on the $^{22}Ne/^{21}Ne$ ratio are underestimating the shielding effects in such a large object. Since the $^{21}Ne/^{26}Al$ production rate ratio is relatively constant, independent of shielding, the $^{21}Ne/^{26}Al$ age is more reliable. After quadratically adding an uncertainty of approximately 10% in the production rate, we adopt a CRE age of 19.5 ± 2.5 Myr for Almahata Sitta.

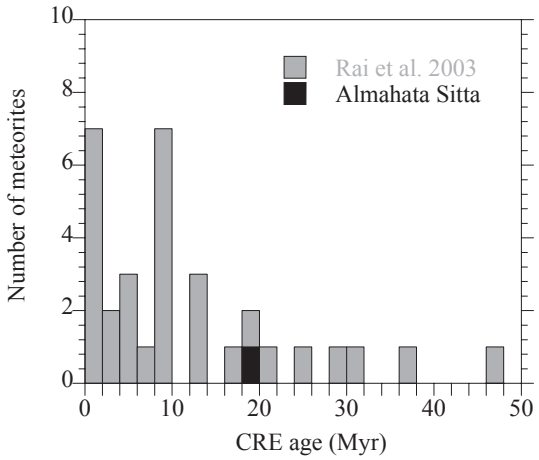

Fig. 8. Histogram of the CRE age of Almahata Sitta (black bar, this work) compared to those of approximately 30 other ureilites (Rai et al. 2003).

The concordant noble gas and $^{21}Ne/^{26}Al$ exposure ages of the four samples and the dependence of the ^{10}Be and ^{26}Al concentrations on the $^{22}Ne/^{21}Ne$ ratio are consistent with a simple exposure history as a large object, thus excluding a significant previous exposure on the parent body. We thus conclude that the CRE age of approximately 20 Myr for Almahata Sitta represents the transfer time of asteroid 2008 TC_3 as a meter-sized body, i.e., after its ejection from a much larger F-type parent body in the asteroid belt, to Earth. Figure 8 shows that the CRE age of the Almahata Sitta ureilite is in the middle of the range of ages of 1–50 Myr for ureilites (Rai et al. 2003), and is not part of a possible cluster at approximately 10 Myr. Considering the high porosity of asteroid 2008 TC_3, a CRE age of approximately 20 Myr may seem surprisingly high for such a fragile object. However, the long survival time of asteroid 2008 TC_3 in space is consistent with impact experiments on porous targets, which suggest that the collisional lifetimes of porous objects are the same or higher than for solid objects (Love et al. 1993; Ryan et al. 1999).

Trapped Noble Gases

Most of our Almahata Sitta samples contain concentrations of trapped ^{36}Ar on the order of 10–100×10^{-8} cm^3 STP g^{-1} (Table 3), in the range typically found for bulk ureilite samples (Göbel et al. 1978; Rai et al. 2003). Sample #44, on the other hand, is unusually rich in ^{36}Ar and correspondingly has a remarkably low $^{40}Ar/^{36}Ar$ ratio of 0.060. It appears possible that this split contained an untypically large proportion of carbon-rich vein material, which is heavily enriched in trapped noble gases (Göbel et al. 1978). The $^{4}He/^{20}Ne$ ratio of approximately 22 and $^{20}Ne/^{36}Ar$ ratio of approximately 0.005 for the trapped component of sample #44 are in the ranges reported for other bulk ureilite samples (Göbel et al. 1978).

The trapped Ne and Ar abundances in two splits of sample #47 show relatively good agreement with those reported by Ott et al. (2010) for their split from the same sample, i.e., the trapped ^{20}Ne and ^{36}Ar concentrations in three splits agree within approximately 25% and approximately 16%, respectively. However, our split of sample #36 shows very different trapped noble gas abundances than those reported by Murty et al. (2010) for their bulk sample of Almahata specimen #36, which is a factor of 3 higher in trapped ^{36}Ar and a factor of approximately 100 higher in trapped ^{20}Ne than our sample. Apparently, sample #36 is more heterogenous than sample #47.

SUMMARY AND CONCLUSIONS

The concentrations of cosmogenic ^{10}Be, ^{26}Al, and ^{36}Cl in six fragments of the Almahata Sitta ureilite strewn field indicate that they came from an object with a radius of approximately 300 g cm^{-2}. Although the absolute size of asteroid 2008 TC_3 is somewhat uncertain due to uncertainties in the average albedo of the asteroid, the effective radius is most likely between 150 and 200 cm, based on the measured albedo of 0.04–0.10 for the recovered meteorites. Given the preatmospheric radius of Almahata Sitta of 180 ± 20 cm as determined from direct observations of the small asteroid before its impact on Earth (assuming an albedo of 0.05), we obtain a bulk density of asteroid 2008 TC_3 of 1.66 g cm^{-3} and a preatmospheric mass to 33,000–51,000 kg. Based on an average grain density of approximately 3.35 g cm^{-3}, the inferred bulk density indicates that asteroid 2008 TC_3 had a bulk porosity of approximately 50%, which corroborates independent estimates of the high porosity based on atmospheric fragmentation (Borovička and Charvat 2009).

The high porosity of asteroid 2008 TC_3 explains the catastrophic disruption at high altitude in Earth's atmosphere. Most of the recovered ureilite fragments have densities in the range of 2.1–3.2 g cm^{-3} (Shaddad et al. 2010), which suggests that the surviving meteorites represent the least porous parts of asteroid 2008 TC_3, which must have been quite heterogeneous in terms of bulk density and bulk porosity. The bulk density of asteroid 2008 TC_3 is on the low end of the range of densities of 1.6–3.7 g cm^{-3} measured for stone meteorites (Consolmagno and Britt 1998; Britt and Consolmagno 2003), but is similar to the value of approximately 1.6 g cm^{-3} determined for the Tagish Lake meteoroid (Hildebrand et al. 2006) and only slightly higher than bulk densities of 1.0–1.5 g cm^{-3} for

several C-type asteroids, which are assumed to be rubble piles (Britt et al. 2002). Although the high porosity of asteroid 2008 TC_3 could be interpreted as an argument for a rubble pile structure, the low densities of some of the recovered meteorites from the Almahata Sitta strewn field suggest that most of the porosity in asteroid 2008 TC_3 is due to microporosity, i.e., cracks and voids on a mm to cm scale, as was observed in thin section (e.g., Shaddad et al. 2010; Zolensky et al. 2010). This implies that not all low-density asteroids are necessarily rubble pile objects.

The cosmogenic ^{21}Ne and ^{26}Al concentrations in four Almahata Sitta fragments yield a CRE age of 19.5 ± 2.5 Myr. The combined cosmogenic noble gas and radionuclide records in Almahata Sitta show no evidence of a previous exposure on the surface of a larger parent body. The CRE age of approximately 20 Myr thus represents the transfer time of asteroid 2008 TC_3 from the time it broke off as a large chunk from an F-class parent body in the asteroid belt, evolved to an orbit in the chaotic resonance zone, and was then perturbed into an eccentric orbit on a collision course with Earth. Combined with orbital dynamics models, the CRE age of Almahata Sitta may provide insight into the location of the parent body of asteroid 2008 TC_3 in the main belt, with the two main candidates being the Polana asteroid family near the 3:1 resonance (Jenniskens et al. 2010) and the Hoffmeister asteroid family near the 5:2 resonance (Migliorini et al. 1996).

Acknowledgments—We thank the students and staff of the University of Khartoum for their efforts in recovering the meteorites and for making samples available for analysis. This work was supported by NASA grant NNG06GF22G and the Swiss National Science Foundation. P. J. is supported by a grant from the Planetary Astronomy program. This paper benefited from constructive reviews by G. Herzog, R. Reedy, and editorial comments by A. J. T. Jull.

Editorial Handling—Dr. A. J. Timothy Jull

REFERENCES

Alexeev V. A. 1998. Parent bodies of L and H chondrites: Times of catastrophic events. *Meteoritics & Planetary Science* 33:145–152.

Aylmer D., Vogt S., Herzog G. F., Klein J., Fink D., and Middleton R. 1990. Low ^{10}Be and ^{26}Al contents in ureilites: Production at meteoroid surfaces. *Geochimica et Cosmochimica Acta* 54:1775–1784.

Berkley J. L., Taylor G. J., and Keil K. 1980. The nature and origin of ureilites. *Geochimica et Cosmochimica Acta* 44:1579–1597.

Bischoff A., Horstmann M., Pack A., Laubenstein M., and Haberer S. 2010. Asteroid 2008 TC_3—Almahata Sitta: A spectacular breccia containing many different ureilitic and chondritic lithologies. *Meteoritics & Planetary Science* 45. This issue.

Borovička J. and Charvat Z. 2009. Meteosat observation of the atmospheric entry of 2008 TC_3 over Sudan and the associated dust cloud. *Astronomy & Astrophysics* 507:1015–1022.

Britt D. T. and Consolmagno G. J. 2003. Stony meteorite porosities and densities: A review of the data through 2001. *Meteoritics & Planetary Science* 38:1161–1180.

Britt D., Yeomans D., Housen K., and Consolmagno G. J. 2002. Asteroid density, porosity and structure. In *Asteroids III*, edited by Paolicchi P. and Binzel R. P. Tucson, AZ: The University of Arizona Press. pp. 485–500.

Cellino A., Zappala V., Doressoundiram A., Di Martino M., Bendjoya Ph., Dotto E., and Migliorini F. 2001. The puzzling case of the Nysa-Polana family. *Icarus* 152:225–237.

Consolmagno G. J. and Britt D. T. 1998. The density and porosity of meteorites from the Vatican collection. *Meteoritics & Planetary Science* 33:1231–1241.

Eberhardt P., Eugster O., and Marti K. 1965. A redetermination of the isotopic composition of atmospheric neon. *Zeitschrift für Naturforschung* 20a:623–624.

Eberhardt P., Eugster O., Geiss J., and Marti K. 1966. Rare gas measurements in 30 stone meteorites. *Zeitschrift für Naturforschung* 21a:414–426.

Eugster O. 1988. Cosmic-ray production rates of ^{3}He, ^{21}Ne, ^{38}Ar, ^{83}Kr and ^{126}Xe in chondrites based on ^{81}Kr-Kr exposure ages. *Geochimica et Cosmochimica Acta* 52:1649–1662.

Friedrich J., Wolf S. F., Rumble D. III., Troiano J., Gagnon C. J. L., Jenniskens P., and Shaddad M. H. 2010. The elemental composition of Almahata Sitta. *Meteoritics & Planetary Science* 45. This issue.

Garrison D., Hamlin S., and Bogard D. 2000. Chlorine abundances in meteorites. *Meteoritics & Planetary Science* 35:419–429.

Göbel R., Ott U., and Begemann F. 1978. On trapped noble gases in ureilites. *Journal of Geophysical Research* 83:855–867.

Graf T., Baur H., and Signer P. 1990. A model for the production of cosmogenic nuclides in chondrites. *Geochimica et Cosmochimica Acta* 54:2521–2534.

Herrin J. S., Zolensky M. E., Ito M., Jenniskens P., and Shaddad M. H. 2009. Fossilized smelting: Reduction textures in Almahata Sitta ureilite (abstract). *Meteoritics & Planetary Science* 44:A227.

Herzog G. F. and Anders E. 1971. Radiation age of the Norton County meteorite. *Geochimica et Cosmochimica Acta* 35:239–244.

Hildebrand A. R., McClausland P. J. A., Brown P. G., Longstaffe F. J., Russell S. D. J., Tagliaferri E., Wacker J. F., and Mazur M. J. 2006. The fall and recovery of the Tagish Lake meteorite. *Meteoritics & Planetary Science* 41:407–431.

Hiroi T., Jenniskens P. M., Bishop J. L., Shatir T. S. M., and Kudoda A. M. 2010. Bidirectional visible-NIR and biconical FT-IR reflectance spectra of Almahata Sitta meteorite samples. *Meteoritics & Planetary Science* 45. This issue.

Hoffmann V. H., Hochleitner R., Torii M., Funaki M., Mikouchi T., and Almahata Sitta Consortium. 2010. Magnetism and mineralogy of Almahata Sitta (abstract

#2120). 41st Lunar and Planetary Science Conference. CD-ROM.

Jenniskens P., Shaddad M. H., Numan D., Elsir S., Kudoda A. M., Zolensky M. E., Le L., Robinson G. A., Friedrich J. M., Rumble D., Steele A., Chesley S. R., Fitzsimmons A., Duddy S., Hsieh H. H., Ramsay G., Brown P. G., Edwards W. N., Tagliaferri E., Boslough M. B., Spalding R. E., Dantowitz R., Kozubal M., Pravec P., Borovička J., Charvat Z., Vaubaillon J., Kuiper J., Albers J., Bishop J. L., Mancinelli R. L., Sandford S. A., Milam S. N., Nuevo M., and Worden S. P. 2009. The impact and recovery of asteroid 2008 TC_3. *Nature* 458:485–488.

Jenniskens P., Vaubaillon J., Binzel R. P., DeMeo F. E., Nesvorny D., Bottke W. F., Fitzsimmons A., Hiroi T., Marchis F., Bishop J. L., Zolensky M. E., Herrin J. S., Welten K. C., Meier M. M. M., Vernazza P., and Shaddad M. H. 2010. Almahata Sitta (= asteroid 2008 TC3) and the search. *Meteoritics & Planetary Science* 45. This issue.

Jenniskens P., Vaubaillon J., Binzel R. P., Fitzsimmons A., Hiroi T., Marchis F., Bishop J., Zolensky M. E., Herrin J. S., and Shaddad M. H. 2010. 2008 TC_3 identifies the Polana family as the ureilite parent body. *Meteoritics & Planetary Science*. This issue.

Kim K. J., Masarik J, and Reedy R. C. 2005. The effects of geometry on nuclide production processes in meteorites (abstract). *Meteoritics & Planetary Science* 40:A80.

Kowalski R. A., Beshore E. C., Boattini A., Garradd G. J., Gibbs A. R., Grauer A. D., Hill R. E., Larson S. M., and McNaught R. H. 2008. Minor Planet Electronic Circular 2008-T50. In edited by Williams G. V. Cambridge, MA, USA.

Leya I. and Masarik J. 2009. Cosmogenic nuclides in stony meteorites revisited. *Meteoritics & Planetary Science* 44:1061–1086.

Leya I., Lange H.-J., Neumann S., Wieler R., and Michel R. 2000. The production of cosmogenic nuclides in stony meteoroids by galactic cosmic ray particles. *Meteoritics & Planetary Science* 35:259–286.

Lingenfelter R. E., Canfield E. H., and Hampel V. E. 1972. The lunar neutron flux revisited. *Earth and Planetary Science Letters* 16:355–369.

Lorenzetti S., Eugster O., Busemann H., Marti K., Burbine T. H., and McCoy T. 2003. History and origin of aubrites. *Geochimica et Cosmochimica Acta* 67:557–571.

Love S. G., Hörz F., and Brownlee D. E. 1993. Target porosity effects in impact cratering and collisional disruption. *Icarus* 105:216–224.

Masarik J. and Reedy R. C. 1994a. Effects of meteoroid shape on cosmogenic nuclide production rates (abstract). 25th Lunar and Planetary Science Conference. pp. 843–844.

Masarik J. and Reedy R. C. 1994b. Effects of bulk composition on nuclide production processes in meteorites. *Geochimica et Cosmochimica Acta* 58:5307–5317.

Migliorini F., Manara A., Di Martino M., and Farinella P. 1996. The Hoffmeister asteroid family: Inferences from physical data. *Astronomy & Astrophysics* 310:681–685.

Murty S. V. S., Mahajan R. R., Jenniskens P., Shaddad M. H., and Eldien B. 2010. Noble gases and nitrogen in the Almahata Sitta ureilite. *Meteoritics & Planetary Science* 45. This issue.

Nagai H., Honda M., Imamura M., and Kobayashi K. 1993. Cosmogenic ^{10}Be and ^{26}Al in metal, carbon and silicate of meteorites. *Geochimica et Cosmochimica Acta* 57:3705–3723.

Nishiizumi K. 2004. Preparation of ^{26}Al AMS standards. *Nuclear Instruments and Methods* B223-224:388–392.

Nishiizumi K., Regnier S., and Marti K. 1980. Cosmic ray exposure ages of chondrites, pre-irradiation and constancy of cosmic ray flux in the past. *Earth and Planetary Science Letters* 56:156–170.

Nishiizumi K., Imamura M., Caffee M. W., Southon J. R., Finkel R. C., and McAninch J. 2007. Absolute calibration of ^{10}Be AMS standards. *Nuclear Instruments and Methods in Physics Research B* 258:403–413.

Ott U. 2002. Noble gases in meteorites—Trapped components. In *Noble gases*, edited by Porcelli D., Ballentine C. J., and Wieler R. Reviews in Mineralogy and Geochemistry, vol. 47, Washington, D.C.: Mineralogical Society of America. pp. 71–100.

Ott U., Herrmann S., Jenniskens P., and Shaddad M. 2010. A noble gas study of two stones from the Almahata Sitta meteorite (abstract #1195). 41st Lunar and Planetary Science Conference. CD-ROM.

Rai V. K., Murty S. V. S., and Ott U. 2003. Noble gases in ureilites: Cosmogenic, radiogenic and trapped components. *Geochimica et Cosmochimica Acta* 67:4435–4456.

Reedy R. C. 1981. Cosmic-ray produced stable nuclides: Various production rates and their implications. Proceedings, 12th Lunar and Planetary Science Conference. pp. 1809–1823.

Rochette P., Gattacceca J., Bourot-Denise M., Consolmagno G., Folco L., Kohout T., Pesonen L., and Sagnotti L. 2009. Magnetic classification of stony meteorites: 3. Achondrites. *Meteoritics & Planetary Science* 44:405–427.

Rubin A. E. and Grossman J. N. 2010. Meteorite and meteoroid: New comprehensive definitions. *Meteoritics & Planetary Science* 45:114–122.

Rumble D., Zolensky M. E., Friedrich J. M., Jenniskens P., and Shaddad M. H. 2010. The oxygen isotope composition of Almahata Sitta. *Meteoritics & Planetary Science* 45. This issue.

Ryan E. V., Davis D. R., and Giblin I. 1999. A laboratory impact study of simulated edgeworth-Kuiper Belt objects. *Icarus* 142:56–62.

Scheirich P., Ďurech J., Pravec P., Kozubal M., Dantowitz R., Kaasalainen M., Betzler A. S., Beltrame P., Muler G., Birtwhistle P., and Kugel F. 2010. The shape and rotation of asteroid 2008 TC_3. *Meteoritics & Planetary Science* 45. This issue.

Shaddad M. H., Jenniskens P., Kudoda A. M., Numan D., Elsir S., Riyad I. F., Ali A. E., Alameen M., Alameen N. M., Eid O., Osman A. T., AbuBaker M. I., Chesley S. R., Chodas P. W., Albers J., Edwards W. N., Brown P. G., Kuiper J., and Friedrich H. 2010. The recovery and characterization of Almahatta Sitta. *Meteoritics & Planetary Science* 45. This issue.

Sharma P., Kubik P. W., Fehn U., Gove G. E., Nishiizumi K., and Elmore D. 1990. Development of ^{36}Cl standards for AMS. *Nuclear Instruments and Methods in Physics Research B* 52:410–415.

Sharma P., Bourgeois M., Elmore D., Granger D., Lipschutz M. E., Ma X., Miller T., Mueller K., Rickey F., Simms P., and Vogt S. 2000. PRIME lab AMS performance, upgrades and research applications. *Nuclear Instruments and Methods in Physics Research B* 172:112–123.

Spergel M. S., Reedy R. C., Lazareth O. W., Levy P. W., and Slatest L. A. 1986. Cosmogenic neutron-capture-produced nuclides in stony meteorites. *Journal of Geophysical Research* 91:D483–D494.

Taricco et al. *Meteoritics & Planetary Science* 45. This issue
Warner B. D., Harris A. W., and Pravec P. 2009. The asteroid lightcurve database. *Icarus* 202:134–146.
Welten K. C., Caffee M. W., Leya I., Masarik J., Nishiizumi K., and Wieler R. 2003. Noble gases and cosmogenic radionuclides in the Gold Basin L4-chondrite shower: Thermal history, exposure history and pre-atmospheric size. *Meteoritics & Planetary Science* 38:157–173.
Welten K. C., Nishiizumi K., Caffee M. W., and Hillegonds D. J. 2006. Cosmogenic radionuclides in ureilites from Frontier Mountain, Antarctica: Evidence for a polymict breccia (abstract #2391). 37th Lunar and Planetary Science Conference. CD-ROM.
Wieler R., Graf T., Pedroni A., Signer P., Pellas P., Fieni C., Suter M., Vogt S., Clayton R. N., and Laul J. C. 1989. Exposure history of the regolithic chondrite Fayetteville: II. Solar-gas-free light inclusions. *Geochimica et Cosmochimica Acta* 53:1449–1459.
Zolensky M. E., Herrin J., Jenniskens P., Friedrich J. M., Rumble D., Steele A., Sandford S. A., Shaddad M. H., Le L., Robinson G. A., and Morris R. V. 2009. Mineralogy of the Almahata Sitta ureilite (abstract). *Meteoritics & Planetary Science* 44:A227.
Zolensky M. E., Herrin J., Mikouchi T., Ohsumi K., Friedrich J., Steele A., Fries M., Sandford S. A., Milan S., Hagiya K., Takeda H., Satake W., Kurihara T., Colbert M., Hanna R., Maisano J., Ketcham R., Le L., Robinson G. A., Martinez J. E., Jenniskens P., and Shaddad M. H. 2010. Mineralogy and petrography of the Almahata Sitta ureilite. *Meteoritics & Planetary Science* 45. This issue.